ANTIMICROBIAL AGENTS AND CHEMOTHERAPY, Sept. 2007, p. 3338–3345 Vol. 51, No. 9
0066-4804/07/$08.00+0 doi:10.1128/AAC.00276-07

Location of Persisting Mycobacteria in a Guinea Pig Model of Tuberculosis Revealed by R207910[▽]

Anne J. Lenaerts,[1]* Donald Hoff,[1] Sahar Aly,[2] Stefan Ehlers,[2] Koen Andries,[3] Luis Cantarero,[4] Ian M. Orme,[1] and Randall J. Basaraba[1]

Department of Microbiology, Immunology and Pathology, Colorado State University, Fort Collins, Colorado 80523[1]; Molecular Infection Biology, Research Center Borstel, Parkallee 22, D-23845 Borstel, Germany[2]; Johnson & Johnson Pharmaceutical Research and Development, Turnhoutseweg 30, 2340 Beerse, Belgium[3]; and Mycos Research, 520 E. 67th Ave., Loveland, Colorado 80538[4]

Received 23 February 2007/Returned for modification 6 April 2007/Accepted 15 May 2007

The lengthy chemotherapy of tuberculosis reflects the ability of a small subpopulation of *Mycobacterium tuberculosis* bacteria to persist in infected individuals. To date, the exact location of these persisting bacteria is not known. Lung lesions in guinea pigs infected with *M. tuberculosis* have striking similarities, such as necrosis, mineralization, and hypoxia, to natural infections in humans. Guinea pigs develop necrotic primary lesions after aerosol infection that differ in their morphology compared to secondary lesions resulting from hematogenous dissemination. In infected guinea pigs conventional therapy for tuberculosis during 6 weeks reduced the bacterial load by 1.7 logs in the lungs and, although this completely reversed lung inflammation associated with secondary lesions, the primary granulomas remained largely unaffected. Treatment of animals with the experimental drug R207910 (TMC207) for 6 weeks was highly effective with almost complete eradication of the bacteria throughout both the primary and the secondary lesions. Most importantly, the few remnants of acid-fast bacilli remaining after R207910 treatment were to be found extracellular, in a microenvironment of residual primary lesion necrosis with incomplete dystrophic calcification. This zone of the primary granuloma is hypoxic and is morphologically similar to what has been described for human lung lesions. These results show that this acellular rim may, therefore, be a primary location of persisting bacilli withstanding drug treatment.

Tuberculosis (TB) is treatable by drugs, and the World Health Organization has promoted the use of "directly observed therapy" to administer effective regimens to infected patients. However, despite this, no new drug classes have been introduced in the last two to three decades and new, effective compounds are badly needed. A central problem, however, even when compliance problems are dealt with, is the sheer length of time needed for current drug regimens to ensure clearance of the infection without relapse (44). As a result, conventional drug regimens are usually of 6 to 9 months in length.

The length of treatment is believed to represent the need to eradicate a small population of bacteria that persist within the lung and extrapulmonary tissues. In addition, these "persisters" likely are the source of reactivation TB that can then occur at a later date, including as a result of human immunodeficiency virus infection. The different mechanisms underlying mycobacterial persistence are not known but appear to represent some form of refractory state rather than true drug resistance (7, 26, 31). In vitro a subpopulation of 5 to 10% of *Mycobacterium tuberculosis* appears far less responsive to killing by drugs. In vivo ca. 99% of bacteria in mice are killed within 2 weeks of drug treatment, but then it requires at least 3 more months of treatment to clear the remaining 1% (19–21, 28, 40). This apparent drug tolerance of *M. tuberculosis* can be readily demonstrated and modeled in mice.

Treatment of persisting bacteria in humans is lengthy and is probably complicated by limited tissue distribution of drugs within encapsulated, calcified lung lesions that develop as the result of a primary infection. Nonprogressive lesions are characterized by well-organized and encapsulated foci of granulomatous inflammation that develop central areas of necrosis and dystrophic mineralization (41). These poorly vascularized lesions are thought to harbor bacilli in certain microenvironments with hypoxic conditions confounding treatment (reviewed in reference 14). The lesions that develop in the guinea pig after low-dose aerosol treatment with *M. tuberculosis* have striking similarities to natural infections in humans, thus making this animal a good model to study bacterial persistence (25, 39). Like humans (41), naive guinea pigs develop primary lesions after initial exposure that differ in their morphology compared to secondary lesions originating from hematogenous dissemination after activation of acquired immunity (24, 33). In addition, guinea pigs, like humans, develop rapidly progressing granulomatous and necrotizing lymphadenitis within lymph nodes that drain the primary lung lesion (5, 6). The characteristic progression of lesion pathology with similarities to those of humans has made the guinea pig model valuable for TB vaccine testing (reviewed in references 23 and 30) and is beginning to be used more frequently for drug testing (18, 35, 36). Persistence caused by certain microenvironmental conditions cannot be modeled in mice since these environmental conditions simply do not occur in *M. tuberculosis*-infected wild-type mice (1, 38).

To further explore the potential of the guinea pig model in drug development, we examined the effects of standard and

* Corresponding author. Mailing address: Department of Microbiology, Immunology and Pathology, Colorado State University, Fort Collins, CO 80523. Phone: (970) 491-3079. Fax: (970) 491-5125. E-mail: lenaerts@colostate.edu.

▽ Published ahead of print on 21 May 2007.

TABLE 1. Bacterial numbers in whole lungs and spleens of drug-treated guinea pigs infected with *M. tuberculosis*

Expt and treatment	Dose (mg/kg)	Lungs			Spleen	
		CFU	Log_{10} CFU ± SEM	n^a	Log_{10} CFU ± SEM	n^a
1						
Sucrose control	None	2.23×10^5	5.48 ± 0.21	5/5	5.94 ± 0.03	5/5
INH-RIF-PZA	10-12-25	5,623	3.75 ± 0.18	5/5	2.27 ± 0.65	5/5
2						
Sucrose control	None	2.23×10^5	5.35 ± 0.42	5/5	5.04 ± 0.47	5/5
R207910	15	46	0.93 ± 0.41	2/5	0.98 ± 0.6	2/5
R207910	10	251	1.29 ± 0.6	2/5	0.46 ± 0.46	1/5
R207910	5	358	2.27 ± 0.3	5/5	0.54 ± 0.54	1/5

[a] *n*, number of guinea pigs showing viable bacteria at time of sacrifice/total number of animals tested. The treatment duration was 6 weeks for all experiments.

experimental chemotherapy in guinea pigs infected by low dose aerosol with the virulent H37Rv strain of *M. tuberculosis*. We assessed the efficacy of these drug therapies in the guinea pig by determining the reduction in bacterial load, by studying the lung histopathology of the primary and secondary granulomas, and by determining the location of the remaining bacilli withstanding drug therapy.

MATERIALS AND METHODS

Bacterial isolate. *M. tuberculosis* H37Rv (Trudeau Institute, Saranac Lake, NY) was grown from low-passage seed lots in Proskauer-Beck liquid medium containing 0.05% Tween 80 to early mid-log phase and frozen in aliquots at −70°C until needed. Cultures were diluted in sterile water prior to use. This isolate is used routinely in our laboratory for guinea pig infection studies (9).

Chemicals and drugs. Isoniazid (INH), rifampin (RIF), and pyrazinamide (PZA) were obtained from Sigma Chemical Co. (St. Louis, MO). RIF was dissolved in 100% dimethyl sulfoxide prior to dilution in distilled water (5% final dimethyl sulfoxide concentration). INH and PZA were dissolved in distilled water. Drug preparations in distilled water were prepared weekly and stored at 4°C. Compound J was prepared at Tibotec (Belgium) monthly in a hydroxypropyl-β-cyclodextrin solution as described before (2). (The solution has been shown by Johnson & Johnson to be 100% chemically stable for a month when kept at 4°C.) All drug doses were prepared with final 40% (wt/vol) sucrose to increase the palatability for the guinea pigs, as is our general procedure.

Animals. Female outbred Hartley guinea pigs (~600 g [body weight]) were purchased from Charles River Laboratories (North Wilmington, MA) and held under barrier conditions in a biosafety level III animal laboratory.

Experimental *M. tuberculosis* infection and chemotherapy. To assess the efficacy of the experimental chemotherapy in guinea pigs, the protocol followed was performed as described before (18). The animals were exposed to an aerosol of *M. tuberculosis* by using a Madison chamber aerosol generation device calibrated to deliver approximately 20 to 30 bacilli into the guinea pig lungs (9). At 30 days postinfection, five guinea pigs were sacrificed to determine the bacterial load at the start of treatment. Subsequently, the animals were allocated into drug groups of five animals each. Animals were treated by administering each dose in the back of the mouth, 5 days per week. Every experiment contained an untreated sucrose control group, i.e., daily oral administration of 1 ml of 40% (wt/vol) sucrose. The standard drug combination of INH-RIF-PZA was administered at 10, 12, and 25 mg/kg, respectively. The doses used here in the guinea pig model do not reflect equipotent doses in TB patients, but doses in the same dose range as R207910, which were found safe in earlier experiments in the guinea pig model. R207910 was formulated in hydroxypropyl-β-cyclodextrin solution administered at 5, 10, or 15 mg/kg in 1 ml of 40% (wt/vol) sucrose. Six days after the completion of chemotherapy (to allow for clearance of drugs in the animals), the animals were sacrificed by sodium barbital injection (Sleepaway; Fort Dodge Laboratories), and the organs were aseptically removed. The right cranial lung lobe (which accounts for 22% of bacterial numbers from whole lungs) was homogenized in 4.5 ml of 0.85% sterile saline with a tissue homogenizer (Kinematic Polytron; Brinkman Instruments Services, Westbury, NY). The number of viable organisms was determined by serial dilution of the homogenates on nutrient LJ agar plates (Difco/Becton Dickinson, Franklin Lakes, NJ) prepared as described by the manufacturer. LJ plates were used to address any carryover of the compound that might be present in the organs at the time of necropsy, as R207910 is a highly protein-bound compound with a long half-life. Initial experiments showed that a serial 1:5 dilution of the homogenates and plating on protein-rich LJ plates dilutes and binds residual compound to an undetectable level (below MIC) that may be present in the organ. The plates were incubated for 3 to 4 weeks at 37°C in ambient air, and viable *M. tuberculosis* CFU were counted. The detection limit of the plating procedure was ~25 CFU, as 1 ml out of 5 ml of the right cranial lung lobe was plated (cranial lung lobe contains ~22% of CFU whole lungs). The viable bacterial counts of whole organs were calculated, converted to logarithms [CFU counts were log-transformed as $\log_{10}(x + 1)$, where x equals the total organ CFU count]. The data were expressed as the mean $\log_{10}$ CFU ± the standard error of the mean for each group.

Statistical analysis. Statistical analysis of CFU data was performed by one-way analysis of variance, followed by an all-pairwise multiple comparison procedure utilizing the Tukey test for the analysis of lung data (SigmaStat v.2.03; SPSS, Inc.).

Histology. After euthanasia, the left cranial lung lobe was infused in situ with 5 ml of 10% neutral-buffered formalin and preserved until processed for histopathological assessment. At the time of processing, all tissues were embedded in paraffin, sectioned at 5 μm, and stained with hematoxylin and eosin (H&E) or stained with acid-fast stain for histologic evaluation and photography. A veterinary pathologist reviewed in a blinded study two serial sections from each guinea pig obtained from equivalent areas of the left cranial lung lobe (section made to obtain largest surface area). Sections stained with H&E were ranked in order of severity on lesion burden by subgross and microscopic examination. The lesion pathology was categorized as mild, moderate, or severe based on a visual estimate of lesion burden. The lesions in the primary granuloma were further categorized based on the type of inflammation and the presence or absence of necrosis, fibrosis, and mineralization. Acid-fast bacilli (AFB) were located by visual inspection of ten random fields, as well as analyzing ten fields at specific locations of the primary granuloma.

Pimonidazole staining. Pimonidazole is a 2-nitroimidazole that has been widely used in tumor biology, where it serves to sensitize tumors for subsequent radiation therapy and is starting to be applied to TB infections (1, 38). The compound is used to determine regions of hypoxia in organs upon injection in the animal. Cells adjacent to areas of necrosis stained markedly with a monoclonal antibody reactive to pimonidazole derivatives known to develop under hypoxia conditions (<4 μM oxygen saturation or prolonged oxygen tensions of 10 mm Hg are required for thiol bonds to be formed) (3, 4). Briefly, 1.5 h prior to sacrifice, guinea pigs were injected intraperitoneally with the hypoxia marker pimonidazole hydrochloride (Chemicon, Hampshire, United Kingdom) in a dose of 60 mg/kg (weight of guinea pig). Sections (2 μm) of formalin-fixed and paraffin-embedded tissues were prepared by using a microtome and were mounted on Superfrost slides (Langenbrinck, Emmendingen, Germany). Antigen retrieval was carried out on deparaffinized tissues with pronase (Fisher Scientific, Schwerte, Germany) for 40 min at 40°C. After reduction of endogenous peroxidase activity with 0.03% hydrogen peroxide for 5 min, the anti-pimonidazole antibody Hypoxyprobe-1MAb1 (dilution 1:50; Chemicon), prelabeled for 15 min with a biotinylation reagent (Dako, Hamburg, Germany) and incubated thereafter for 5 min with a blocking reagent (Dako), was applied to the slides for 15 min. The reaction was visualized by using streptavidin conjugated to horseradish peroxidase.

RESULTS

Chemotherapy of *M. tuberculosis*-infected guinea pigs. The efficacy of the standard combination regimen for TB and the experimental drug R207910 (TMC207) were evaluated in guinea pigs infected with *M. tuberculosis* via a low-dose aerosol (LDA) infection. At the start of treatment (30 days postinfection), the bacterial load in the lungs reached approximately 6 $\log_{10}$ CFU in the lungs. At the completion of the study (after 6 weeks of treatment), the bacterial load in the sucrose control group was between 5.35 to 5.48 $\log_{10}$ CFU (Table 1). In the two experiments presented here, there was a significant reduction of the bacterial load in the lungs of all drug-treated groups versus the sucrose control groups after 6 weeks of therapy ($P < 0.05$) (Table 1).

In a first study, the drug combination of INH at 10 mg/kg, RIF at 12 mg/kg, and PZA at 25 mg/kg reduced the bacterial load by about 1.75 logs in the lungs versus the sucrose controls (reduction of ~98% bacilli). In spleens, a reduction of 3.67 logs was observed versus the untreated control group. In a second study, R207910 (TMC207) was tested at 5, 10, or 15 mg/kg for 6 weeks and showed a strong activity by almost completely eradicating the bacilli throughout the lung tissues. Only very low bacterial numbers (<400 CFU) could be isolated for all R207910 treatment groups (reduction of 99.5% of the bacilli). For the 10- and 15-mg/kg R207910 groups, only two of five guinea pigs showed bacterial growth (Table 1). All remaining colonies tested were found to be drug susceptible by MIC testing (15) for R207910 activity. The detection limit of the present study is ~25 CFU (1 out of 5 ml of the right cranial lung lobe homogenate is plated; the cranial lung lobe is 22% of the total lung). A slight dose response in the R207910 treatment groups can be observed for the three doses tested (Table 1), although care should be taken interpreting these very low bacterial numbers. In spleens, the bacterial numbers of the R207910 group were very low in all groups, with only one or two animals of the treatment groups showing any bacterial growth at all.

Histopathology data of drug-treated, *M. tuberculosis*-infected guinea pigs. Lung lesions in the guinea pig resulting from the initial exposure to *M. tuberculosis* differ from those resulting from hematogenous dissemination which occurs after immune activation. The primary lesions are discrete encapsulated foci of mixed inflammation with central necrosis that progresses to dystrophic mineralization. These lesions are easily differentiated from secondary lesions which are multifocal to coalescing throughout the parenchyma and are composed predominantly of lymphocytes and fewer macrophages and are devoid of necrosis and mineralization (Fig. 1).

Prior to treatment (at 1 month after LDA infection), both primary and secondary granulomas were present in the lungs of the infected guinea pigs of the pretreatment control group (data not shown). Combination therapy with INH, RIF, and PZA, as well as with R207910 did not show any significant effect on the morphology of primary lesions but appeared to result in a complete resolution of the secondary inflammatory lesions. The lack of secondary lesions after drug treatment appeared to be a resolution of existing lesions, as well as the prevention of the development of new secondary lesions. Figure 2 shows that primary lesions are encapsulated by a relatively hypocellular fibrous capsule that delineated the lesions from more normal pulmonary parenchyma. The center of the lesions was found to be hypocellular with necrotic cellular debris with the prominent mineralization at the lesion center, which was delineated from the capsule by a rim of necrotic cellular debris (Fig. 3).

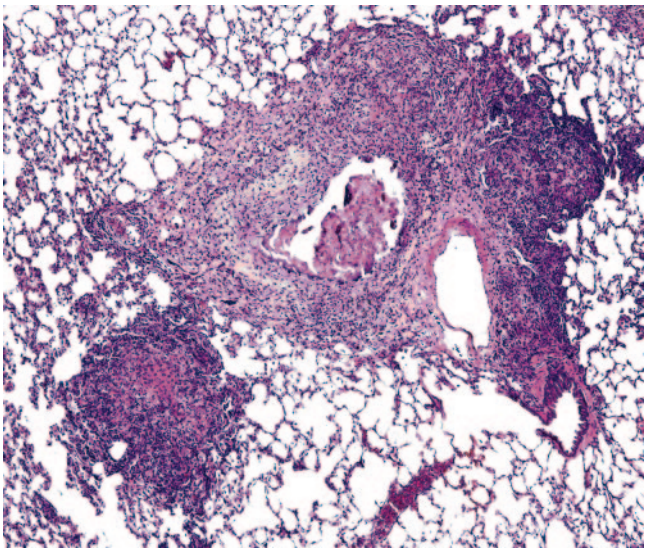

FIG. 1. Lungs from an *M. tuberculosis*-infected guinea pig showing primary and secondary lung lesions. A residual primary lung lesion with dystrophic calcification, which is surrounded by mixed inflammation representing secondary lesions resulting from hematogenous dissemination and inflammation, is shown. Magnification, ×100 (H&E stain).

Acid-fast staining of lung section from untreated guinea pigs showed the presence of mainly intracellular bacilli in the secondary lesions, while in the primary lesions the bacilli appeared to be primarily extracellular within the uncalcified or partially calcified necrotic debris of the primary granuloma (data not shown). Guinea pigs treated with the INH-RIF-PZA combination or with R207910 had morphologically intact AFB remaining within primary lung lesions (Fig. 4). The individual and microcolonies of bacilli in the R207910 group were mainly found extracellularly within the acidophilic acellular rim of the unmineralized residual necrosis of the primary lesions (Fig. 4). After drug treatment no organisms were visible intracellularly within the capsule, and none were present within the normal perilesional parenchyma (not shown).

Staining of hypoxic regions in organs of *M. tuberculosis*-infected guinea pigs with pimonidazole. To determine the hypoxic regions in the organs of guinea pigs infected with *M. tuberculosis*, the animals were injected intraperitoneally with the hypoxia marker 2-nitroimidazole, pimonidazole, 1.5 h before sacrifice. This procedure was performed on groups of guinea pigs 1, 2, and 4 months postinfection by low-dose aerosol with *M. tuberculosis*. Cells in regions of hypoxia stained markedly with a monoclonal antibody reactive to pimonidazole derivatives known to develop under conditions of hypoxia. Staining for hypoxia was detected from 1 month postinfection in the guinea pigs and was more pronounced in the later stages of *M. tuberculosis* infection. Figure 5A shows a typical primary granuloma in lungs from a guinea pig 4 months after infection,

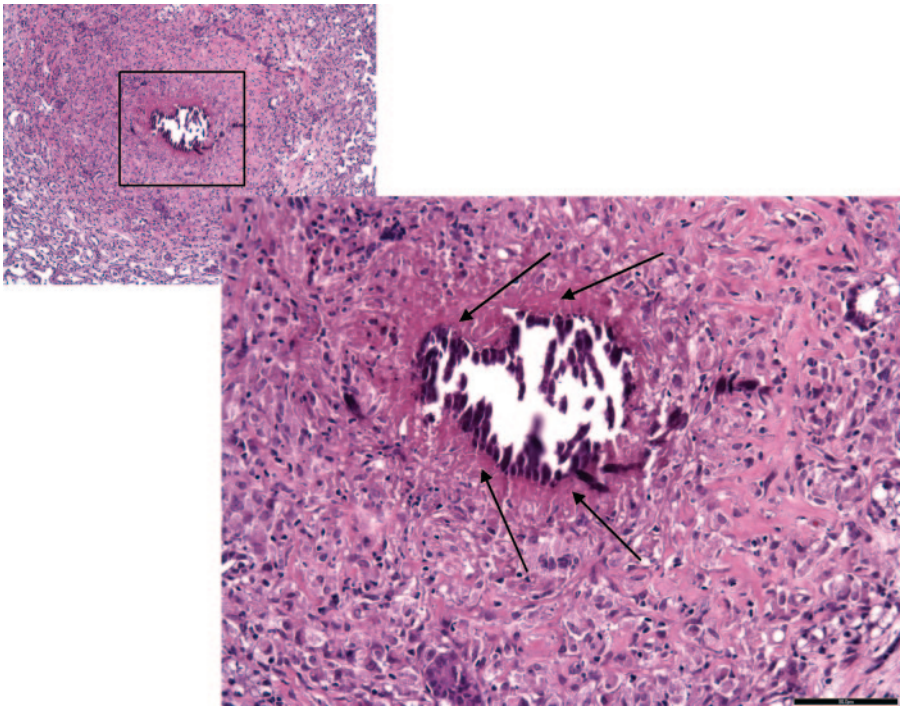

FIG. 2. Primary granuloma in the lungs of *M. tuberculosis*-infected guinea pigs after INH-RIF-PZA drug treatment. The image shows a lung from an *M. tuberculosis*-infected guinea pig treated for 6 weeks with the combination treatment of INH-RIF-PZA; a residual primary lung lesion is evidenced by central necrosis with dystrophic calcification. The lesion is delineated from the normal lung parenchyma by a noncalcified, acellular rim (arrows). The surrounding lung tissue is free of secondary inflammation which is extensive in untreated controls. Magnification ×100 for small inset; magnification ×200 for the large image (H&E stain).

where the center of the lesion is hypocellular with central necrosis and is in the early stages of dystrophic mineralization. The periphery of the necrotic center in the primary granuloma was clearly hypoxic, as demonstrated by its staining with a monoclonal antibody specific for pimonidazole adducts (Fig. 5A to C). Similar hypoxic conditions were seen in regions of severe necrosis in the draining lymph nodes (Fig. 5D and E). Hypoxia was primarily visible in surrounding regions of central necrosis (necrotic areas themselves cannot be stained by pimonidazole due to the lack of live cells that are necessary for the compound to form adducts with).

DISCUSSION

Theoretically, targeting and eradicating persistent bacteria should result in shortening the duration of therapy for TB and may cure a latent infection. To reach this goal, there is an urgent need to identify new TB drugs with potent sterilizing activity against persisting bacteria found in human lungs. With a number of promising TB drug candidates in the pipeline, it is more important than ever to establish an animal model that can evaluate the sterilizing properties of novel TB drug leads. In these studies, we address both aspects. We demonstrate the potent sterilizing activity of the novel R207910 drug candidate against *M. tuberculosis* in the guinea pig model. In addition, R207910 was used here to evaluate the potential of the guinea pig model for testing the sterilizing activity of new drugs against persistent *M. tuberculosis*.

In the present study, the guinea pig model was used in an initial experiment to evaluate the activity of conventional INH, RIF, and PZA chemotherapy. In addition, given recent data (2, 22) showing high activity of a new diarylquinoline R207910 (TMC207) against *M. tuberculosis* in mice, guinea pigs were treated with this drug in a second experiment. In guinea pigs treated with the conventional drugs, the CFU recovered in lungs were about 1.75 logs lower than the sucrose control group and were associated with a complete resolution of secondary lesions, but with no apparent effects on the histopathology of the more developed primary lesions. These results are in keeping with classical studies by Smith et al., who showed that INH, RIF, and PZA chemotherapy sterilized secondary lesions but had far less effect on the primary lesions in guinea pigs (33). A closer examination of their data shows biphasic killing kinetics of the drugs in the primary lesions, which is consistent with the presence of a bacterial subpopulation less responsive to drug treatment (33).

Guinea pigs treated instead with the experimental compound R207910 at 15 mg/kg showed a nearly complete resolution of disease after 6 weeks treatment. Only a few bacterial colonies were found in two out of five guinea pigs showing viable *M. tuberculosis* (a mean of 46 bacilli cultured from whole lungs plated). Hence, R207910 can be regarded as a highly active drug but was not completely sterilizing with the doses and length of treatment used here. The compound is a diarylquinoline targeting the proton pump ATP synthase (2, 17, 22) and is currently in phase II clinical trials. In mice, R207910 was shown to be 10-fold more active than INH and RIF in terms of bactericidal activity (2, 22). This extraordinary

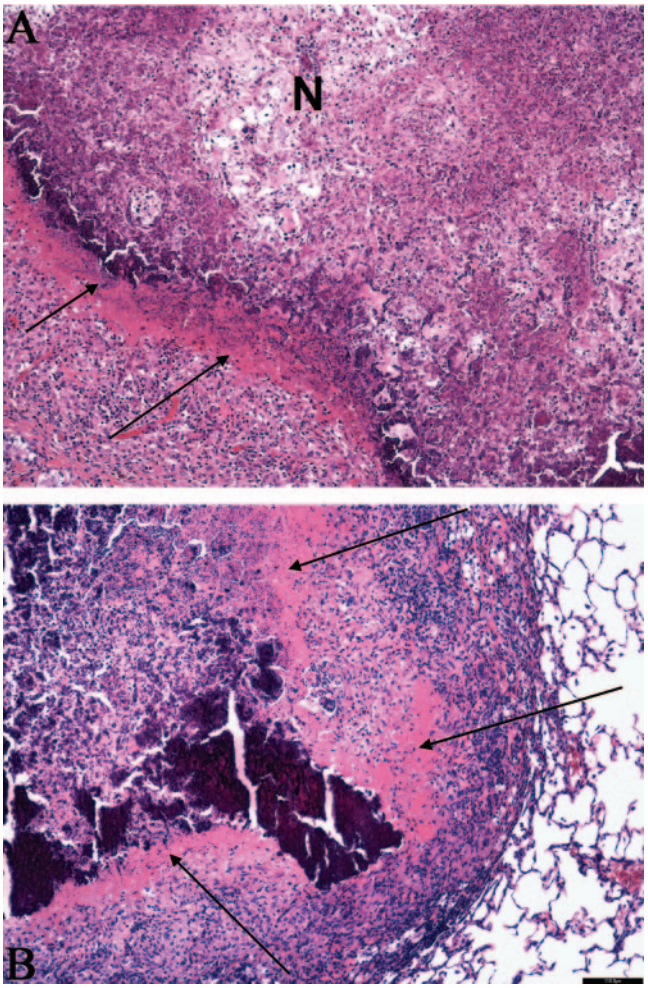

FIG. 3. Detail of the acellular rim delineating the calcified center of the primary granuloma. (A) High magnification of a primary lesion from lungs of an *M. tuberculosis*-infected guinea pig treated for 6 weeks with the combination therapy INH-RIF-PZA. The residual primary lung lesion is evidenced by central necrosis with incomplete dystrophic calcification (indicated by an "N"). Calcified necrotic debris is the granular basophilic material that forms a well-delineated margin from an acellular, rim (arrows) that blends with the fibrous capsule that contains predominantly lymphocytes and fewer macrophages. The lesion is well delineated from the normal lung parenchyma by a fibrous capsule. Magnification, ×200 (H&E stain). (B) Another high-magnification image of a primary lung lesion from an INH-RIF-PZA treated guinea pig infected with *M. tuberculosis*. The lesion shows extensive calcification and still has an acellular, rim (arrow) that blends with the fibrous capsule that contains predominantly lymphocytes and fewer macrophages. More normal lung parenchyma is seen at the section margins. Magnification, ×200 (H&E stain).

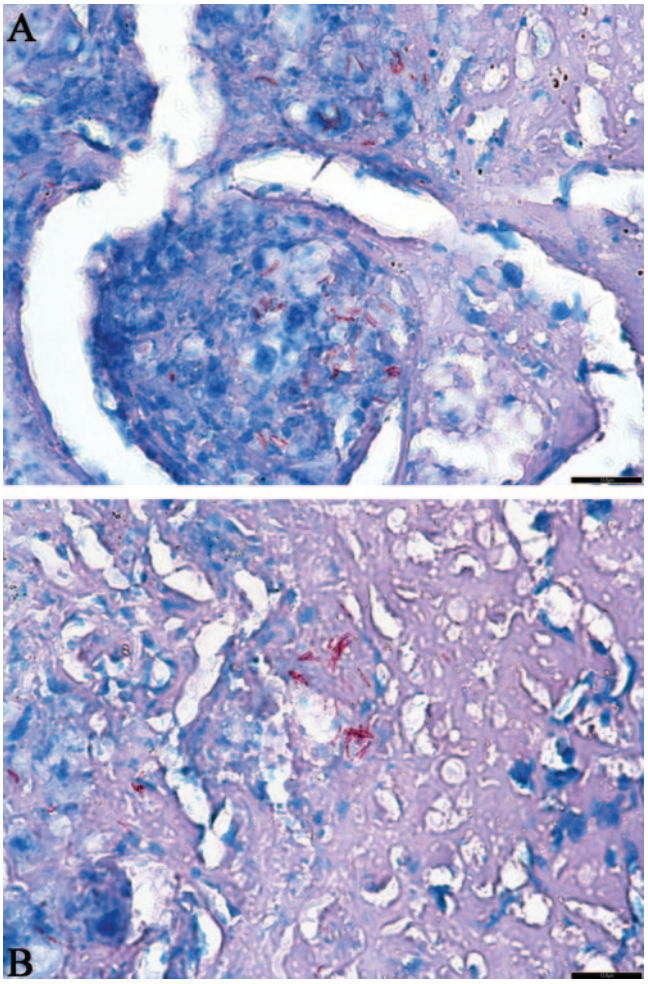

FIG. 4. Location of AFB in the acellular rim of the primary granuloma. (A and B). Primary lung lesion of an *M. tuberculosis*-infected guinea pig treated for 6 weeks with R207610; extracellular AFB (stained in red) are in microcolonies primarily within the acellular, uncalcified remnant of necrosis and to a lesser extent within the central area of partially calcified lytic necrosis. (A) The remaining AFB are extracellular in between lymphocytes and macrophages. (B) The remaining AFB are present in a complete acellular region. Magnification, ×400 (acid fast staining).

potency of R207910 over conventional TB drugs seems to be even more pronounced in the guinea pig model. Hence, the demonstration of high antibacterial activity of R207910 in this second animal model, which develops a heterogeneity of lesions with both intra- and extracellular bacilli, confirms that R207910 might hold great promise as a new TB drug.

To localize the remaining bacilli after drug treatment in the lung lesions, we used acid-fast staining, which is the standard method of detecting mycobacteria in tissues (34). In *M. tuberculosis*-infected but untreated guinea pigs, AFB were found in an intracellular state throughout the secondary lesions, whereas in the primary lesions AFB were found to be primarily extracellular within the uncalcified residual necrosis. After drug treatment some AFB could be found in the central necrotic region of the primary lung granulomas, but the majority were found in a defined, acellular rim between the central mineralized region of the lesion and the foamy macrophage layer delineating the capsule (now heavily compressed by the expanding mineralization). This was observed for both the INH-RIF-PZA treated guinea pigs, as well as for the R207910 group. Interestingly, these foci of AFB in the rim could also be seen after R207910 treatment where only 0.1 to 0.3% of the bacilli survived drug treatment. Treatment with this potent drug thus identified the rim of the necrotic region as a primary location of a bacterial subpopulation able to withstand drug treatment. The number of AFB seen in the lung sections

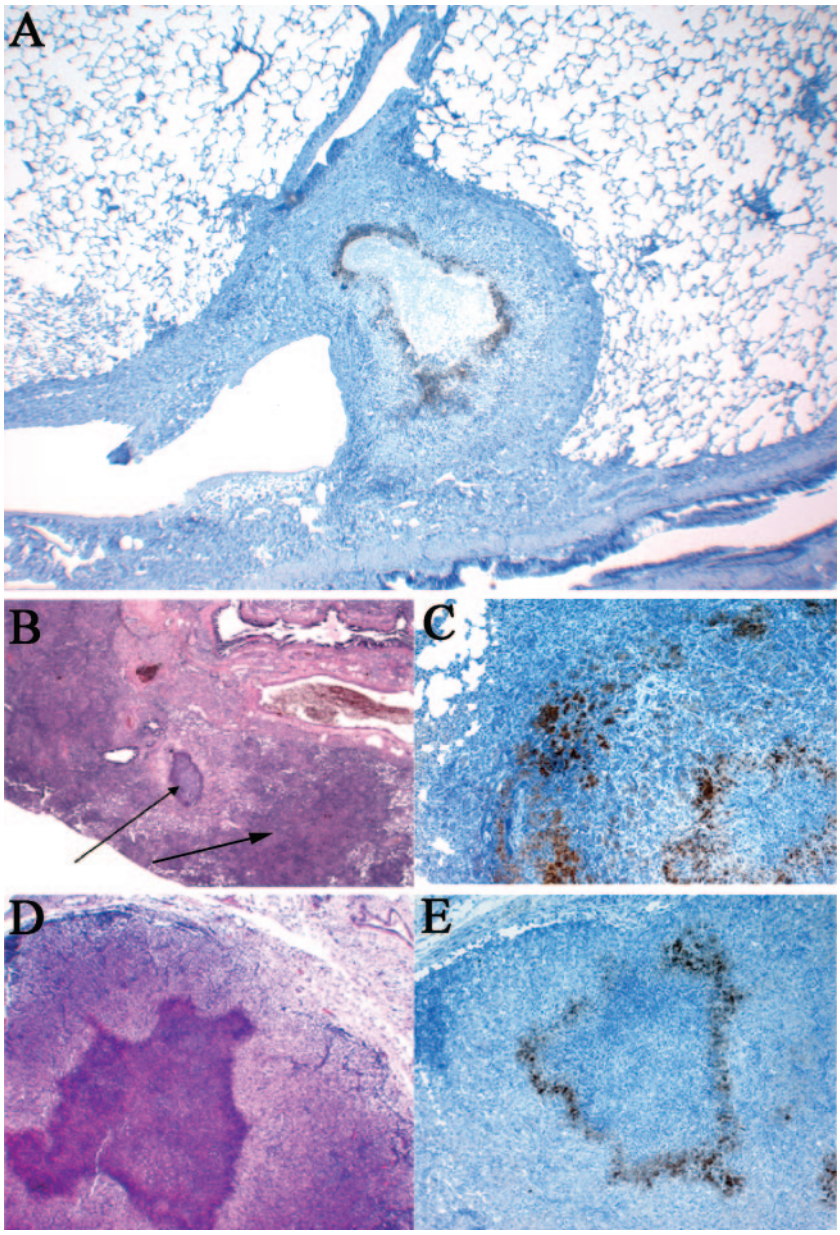

FIG. 5. Lungs and mesenteric lymph nodes from guinea pigs showing the hypoxic regions in the primary granulomas 4 months after *M. tuberculosis* infection. (A) Residual primary lung lesion near a major airway with central necrosis surrounded by epithelioid macrophages that are stained by immunohistochemistry for pimonidazole adducts. The center of the lesion, likely hypoxic, fails to stain due to the lack of viable cells. Magnification, ×40 (hematoxylin counterstain). (B) Residual primary lung lesion with dystrophic calcification and secondary lesion resulting from hematogenous dissemination and inflammation Magnification, ×40 (H&E stain), both indicated by arrows. (C) Primary lung lesion with central necrosis surrounded by epithelioid macrophages that are stained by immunohistochemistry for pimonidazole adducts. Magnification, ×100 (hematoxylin counterstain). (D) Mediastinal lymph node where the normal architecture is replaced by mixed inflammation composed primarily of macrophages and with an extensive, central focus of lytic necrosis. Magnification, ×40 (H&E stain). (E) Mediastinal lymph node with the area of central necrosis surrounded by epithelioid macrophages that are stained by immunohistochemistry for pimonidazole adducts. The center of the lesion, likely hypoxic, fails to stain due to the lack of viable cells (necrosis). Magnification, ×40 (hematoxylin counterstain).

clearly exceeds the number of bacteria cultured after plating of lung homogenates. Therefore, it is reasonable to assume that some of these represent dead bacilli that still retained their morphology, which is consistent with the fact that this drug is a metabolic inhibitor rather than an inhibitor of cell wall biosynthesis. In addition, a proportion of the AFB might be viable but unable to resuscitate growth on bacterial plates. Future studies will address the live-versus-dead-bacteria question in more detail via in situ hybridization using probes for mycobacterial mRNA.

Of great significance, the morphology of the necrotic granulomas in the guinea pig (including the rim delineating the mineralized core), as well as the location of the bacteria, show a strong similarity with human lesions (24, 33, 41). In earlier

studies, mycobacterial material was detected in human lung samples within the central necrosis area and on the periphery of the core by immunohistological staining (42) and by in situ hybridization in the lymphocyte cuff around the central caseous necrosis (13). In human tissues, granulomas undergoing caseous necrosis are characterized by a lack of vascularity, which may lead to decreased oxygen tension or hypoxia (8, 12). A similar lack of vascularity is seen in the primary granulomas in *M. tuberculosis*-infected guinea pigs. This led us to investigate the oxygen tension in tissues of *M. tuberculosis*-infected guinea pigs by injecting pimonidazole, a 2-nitroimidazole that forms covalent bonds in regions of hypoxia. Other researchers have validated this method in the context of TB infections (1, 39). Hypoxia has been postulated as one of the environmental conditions that transitions mycobacteria into a nonreplicating phase, thereby affecting their responsiveness to drugs (11, 43). In the present study a clear hypoxic region was found at the periphery of the necrotic center in the primary granuloma. The center of the primary lesion itself is hypocellular with central necrosis and in the early stages of dystrophic mineralization. The inability of pimonidazole to stain necrotic tissue is due to the lack of viable cells, but this area is also likely to be hypoxic. Of significance, it was within this hypoxic, acellular rim of the primary granuloma where we found the remaining AFB residing in the lung after drug treatment. The hypoxic rim was visible by 30 days after aerosol infection, which indicates that its establishment is an early event. Similar hypoxic conditions were seen in regions of severe necrosis in the draining lymph nodes. Hypoxia was found to be completely absent in the mouse model of *M. tuberculosis* (1, 38). Therefore, caution should be exercised in using the mouse model for testing of novel anti-TB compounds for sterilizing efficacy against a diversity of *M. tuberculosis* phenotypic subpopulations. Mouse models have proven to provide useful information regarding aspects such as absorption, bioavailability, tissue distribution, and the in vivo efficacy of experimental therapeutics. We believe that the guinea pig model might be a valuable addition for advanced testing of drug leads to define their sterilizing properties in a second animal model, presenting a heterogeneity of TB lesions.

The presence of bacteria after drug treatment in the rim around the necrotic center raises the question of whether physical barriers might have had an impact on the penetration of the drug, thereby reducing the drug effect in less-accessible regions of the lung. The studies using pimonidazole indicate that a heterocyclic compound is able to penetrate to the most hypoxic regions in the guinea pig lung and other organs. Drug penetration is, however, dependent on the specific physicochemical parameters of the tested drug, and to identify accurate drug levels in granulomas advanced techniques such as quantitative multi-isotope imaging mass spectrometry would have to be applied. However, the lack of AFB inside the necrotic region after drug treatment suggests that the primary granuloma was permeable to the drugs tested here.

The distinct acellular rim of the primary granuloma harbored large numbers of acid-fast staining bacteria, many of which were present in microcolonies or clusters. All were extracellular and primarily dispersed throughout this region. It is interesting to speculate whether these extracellular bacteria are in what might be some form of a biofilm. This possibility has yet to be considered in terms of *M. tuberculosis*, but it has been noticed that *M. smegmatis* can form biofilms and that this is associated with an altered mycolate profile and an unusual buildup of short-chain fatty acids modulated by GroEL, a major chaperonin (29, 32, 37, 47). Other studies have shown that strains of *M. avium* also have this property (10, 45, 46). Therefore, it is possible that during the progression of a TB infection some bacteria become deprived of their favored intracellular niche as a result of cellular necrosis and, finding themselves in the extracellular fluid form some sort of biofilm, in turn induce genetic mechanisms favoring persistence as an effort to ensure survival.

The findings presented here have important implications in developing sterilizing chemotherapy, as well for evaluating putative mechanisms of latency of *M. tuberculosis* in an in vivo model. Clearly, much more information is needed about this specific microenvironment in the granuloma, and the adaptations used by the bacteria present here to survive. A further intriguing question is whether there are other environments that exhibit similar problems with persistence but with less obvious pathological features as overt necrosis, such as in adipose tissue (27), lymphatics (6), or nontypical host cells (16). Such information could be crucial to developing new sterilizing drugs that can penetrate into sanctuaries where the persistent bacteria reside and hence reduce the duration of therapy.

ACKNOWLEDGMENTS

We thank Veronica Gruppo and Christine Johnson for excellent technical support, and we acknowledge the staff of the Laboratory Animal Resources (Colorado State University) for animal care.

Financial support was provided by the National Institutes of Health research and development contract NO1 AI-95385 (Tuberculosis Antimicrobial Acquisition and Coordinating Facility [Barbara Laughon and Robert Goldman, Project Officers]) and National Institutes of Health grants to I.M.O. (AI054697 and AI070456).

REFERENCES

1. **Aly, S., K. Wagner, C. Keller, S. Malm, A. Malzan, S. Brandau, F. C. Bange, and S. Ehlers.** 2006. Oxygen status of lung granulomas in *Mycobacterium tuberculosis*-infected mice. J. Pathol. **210:**298–305.
2. **Andries, K., P. Verhasselt, J. Guillemont, H. W. Gohlmann, J. M. Neefs, H. Winkler, J. Van Gestel, P. Timmerman, M. Zhu, E. Lee, P. Williams, D. de Chaffoy, E. Huitric, S. Hoffner, E. Cambau, C. Truffot-Pernot, N. Lounis, and V. Jarlier.** 2005. A diarylquinoline drug active on the ATP synthase of *Mycobacterium tuberculosis*. Science **307:**223–227.
3. **Arteel, G. E., R. G. Thurman, and J. A. Raleigh.** 1998. Reductive metabolism of the hypoxia marker pimonidazole is regulated by oxygen tension independent of the pyridine nucleotide redox state. Eur. J. Biochem. **253:**743–750.
4. **Arteel, G. E., R. G. Thurman, J. M. Yates, and J. A. Raleigh.** 1995. Evidence that hypoxia markers detect oxygen gradients in liver: pimonidazole and retrograde perfusion of rat liver. Br. J. Cancer **72:**889–895.
5. **Basaraba, R. J., D. D. Dailey, C. T. McFarland, C. A. Shanley, E. E. Smith, D. N. McMurray, and I. M. Orme.** 2006. Lymphadenitis as a major element of disease in the guinea pig model of tuberculosis. Tuberculosis **86:**386–394.
6. **Basaraba, R. J., E. E. Smith, C. A. Shanley, and I. M. Orme.** 2006. Pulmonary lymphatics are primary sites of *Mycobacterium tuberculosis* infection in guinea pigs infected by aerosol. Infect. Immun. **74:**5397–5401.
7. **Bishai, W. R.** 2000. Rekindling old controversy on elusive lair of latent tuberculosis. Lancet **356:**2113–2114.
8. **Boshoff, H. I., and C. E. Barry III.** 2005. Tuberculosis: metabolism and respiration in the absence of growth. Nat. Rev. Microbiol. **3:**70–80.
9. **Brandt, L., Y. A. Skeiky, M. R. Alderson, Y. Lobet, W. Dalemans, O. C. Turner, R. J. Basaraba, A. A. Izzo, T. M. Lasco, P. L. Chapman, S. G. Reed, and I. M. Orme.** 2004. The protective effect of the *Mycobacterium bovis* BCG vaccine is increased by coadministration with the *Mycobacterium tuberculosis* 72-kilodalton fusion polyprotein Mtb72F in *M. tuberculosis*-infected guinea pigs. Infect. Immun. **72:**6622–6632.
10. **Carter, G., M. Wu, D. C. Drummond, and L. E. Bermudez.** 2003. Characterization of biofilm formation by clinical isolates of *Mycobacterium avium*. J. Med. Microbiol. **52:**747–752.

11. **Cho, S. H., S. Warit, B. Wan, C. H. Hwang, G. F. Pauli, and S. G. Franzblau.** 2007. Low-oxygen-recovery assay for high-throughput screening of compounds against nonreplicating *Mycobacterium tuberculosis*. Antimicrob. Agents Chemother. **51:**1380–1385.
12. **Dannenberg, A. M., and G. A. W. Rook.** 1994. Pathogenesis of pulmonary tuberculosis: an interplay of tissue-damaging and macrophage-activating immune responses—dual mechanisms that control bacillary multiplication, p. 459–483. *In* B. R. Bloom (ed.), Tuberculosis: pathogenesis, protection, and control. ASM Press, Washington, DC.
13. **Fenhalls, G., L. Stevens-Muller, R. Warren, N. Carroll, J. Bezuidenhout, P. Van Helden, and P. Bardin.** 2002. Localisation of mycobacterial DNA and mRNA in human tuberculous granulomas. J. Microbiol. Methods **51:**197–208.
14. **Gomez, J. E., and J. D. McKinney.** 2004. *Mycobacterium tuberculosis* persistence, latency, and drug tolerance. Tuberculosis **84:**29–44.
15. **Gruppo, V., C. M. Johnson, K. S. Marietta, H. Scherman, E. E. Zink, D. C. Crick, L. B. Adams, I. M. Orme, and A. J. Lenaerts.** 2006. Rapid microbiologic and pharmacologic evaluation of experimental compounds against *Mycobacterium tuberculosis*. Antimicrob. Agents Chemother. **50:**1245–1250.
16. **Hernandez-Pando, R., M. Jeyanathan, G. Mengistu, D. Aguilar, H. Orozco, M. Harboe, G. A. Rook, and G. Bjune.** 2000. Persistence of DNA from *Mycobacterium tuberculosis* in superficially normal lung tissue during latent infection. Lancet **356:**2133–2138.
17. **Ibrahim, M., K. Andries, N. Lounis, A. Chauffour, C. Truffot-Pernot, V. Jarlier, and N. Veziris.** 2007. Synergistic activity of R207910 combined with pyrazinamide against murine tuberculosis. Antimicrob. Agents Chemother. **51:**1011–1015.
18. **Johnson, C. M., R. Pandey, S. Sharma, G. K. Khuller, R. J. Basaraba, I. M. Orme, and A. J. Lenaerts.** 2005. Oral therapy using nanoparticle encapsulated anti-tuberculosis drugs in guinea pigs infected with *Mycobacterium tuberculosis*. Antimicrob. Agents Chemother. **49:**4335–4338.
19. **Karakousis, P. C., T. Yoshimatsu, G. Lamichhane, S. C. Woolwine, E. L. Nuermberger, J. Grosset, and W. R. Bishai.** 2004. Dormancy phenotype displayed by extracellular *Mycobacterium tuberculosis* within artificial granulomas in mice. J. Exp. Med. **200:**647–657.
20. **Lamichhane, G., S. Tyagi, and W. R. Bishai.** 2005. Designer arrays for defined mutant analysis to detect genes essential for survival of *Mycobacterium tuberculosis* in mouse lungs. Infect. Immun. **73:**2533–2540.
21. **Lenaerts, A. J., V. Gruppo, K. S. Marietta, C. M. Johnson, D. K. Driscoll, N. M. Tompkins, J. D. Rose, R. C. Reynolds, and I. M. Orme.** 2005. Preclinical testing of the nitroimidazopyran PA-824 for activity against *Mycobacterium tuberculosis* in a series of in vitro and in vivo models. Antimicrob. Agents Chemother. **49:**2294–2301.
22. **Lounis, N., N. Veziris, A. Chauffour, C. Truffot-Pernot, K. Andries, and V. Jarlier.** 2006. Combinations of R207910 with drugs used to treat multidrug-resistant tuberculosis have the potential to shorten treatment duration. Antimicrob. Agents Chemother. **50:**3543–3547.
23. **McMurray, D. N.** 2001. Disease model: pulmonary tuberculosis. Trends Mol. Med. **7:**135–137.
24. **McMurray, D. N.** 2003. Hematogenous reseeding of the lung in low-dose, aerosol-infected guinea pigs: unique features of the host-pathogen interface in secondary tubercles. Tuberculosis **83:**131–134.
25. **McMurray, D. N., F. M. Collins, A. M. Dannenberg, Jr., and D. W. Smith.** 1996. Pathogenesis of experimental tuberculosis in animal models. Curr. Top. Microbiol. Immunol. **215:**157–179.
26. **Munoz-Elias, E. J., J. Timm, T. Botha, W. T. Chan, J. E. Gomez, and J. D. McKinney.** 2005. Replication dynamics of *Mycobacterium tuberculosis* in chronically infected mice. Infect. Immun. **73:**546–551.
27. **Neyrolles, O., R. Hernandez-Pando, F. Pietri-Rouxel, P. Fornes, L. Tailleux, J. A. Payan, E. Pivert, Y. Bordat, D. Aguilar, M. C. Prevost, C. Petit, and B. Gicquel.** 2006. Is adipose tissue a place for *Mycobacterium tuberculosis* persistence? PLoS ONE **1:**e43.
28. **Nuermberger, E. L., T. Yoshimatsu, S. Tyagi, R. J. O'Brien, A. N. Vernon, R. E. Chaisson, W. R. Bishai, and J. H. Grosset.** 2004. Moxifloxacin-containing regimen greatly reduces time to culture conversion in murine tuberculosis. Am. J. Respir. Crit. Care Med. **169:**421–426.
29. **Ojha, A., M. Anand, A. Bhatt, L. Kremer, W. R. Jacobs, Jr., and G. F. Hatfull.** 2005. GroEL1: a dedicated chaperone involved in mycolic acid biosynthesis during biofilm formation in mycobacteria. Cell **123:**861–873.
30. **Orme, I. M.** 2005. Current progress in tuberculosis vaccine development. Vaccine **23:**2105–2108.
31. **Parrish, N. M., J. D. Dick, and W. R. Bishai.** 1998. Mechanisms of latency in *Mycobacterium tuberculosis*. Trends Microbiol. **6:**107–112.
32. **Rose, L., S. H. Kaufmann, and S. Daugelat.** 2004. Involvement of *Mycobacterium smegmatis* undecaprenyl phosphokinase in biofilm and smegma formation. Microbes Infect. **6:**965–971.
33. **Smith, D. W., V. Balasubramanian, and E. Wiegeshaus.** 1991. A guinea pig model of experimental airborne tuberculosis for evaluation of the response to chemotherapy: the effect on bacilli in the initial phase of treatment. Tubercle **72:**223–231.
34. **Somoskovi, A., J. E. Hotaling, M. Fitzgerald, D. O'Donnell, L. M. Parsons, and M. Salfinger.** 2001. Lessons from a proficiency testing event for acid-fast microscopy. Chest **120:**250–257.
35. **Stover, C. K., P. Warrener, D. R. VanDevanter, et al.** 2000. A small-molecule nitroimidazopyran drug candidate for the treatment of tuberculosis. Nature **405:**962–966.
36. **Suarez, S., P. O'Hara, M. Kazantseva, C. E. Newcomer, R. Hopfer, D. N. McMurray, and A. J. Hickey.** 2001. Respirable PLGA microspheres containing rifampicin for the treatment of tuberculosis: screening in an infectious disease model. Pharm. Res. **18:**1315–1319.
37. **Teng, R., and T. Dick.** 2003. Isoniazid resistance of exponentially growing *Mycobacterium smegmatis* biofilm culture. FEMS Microbiol. Lett. **227:**171–174.
38. **Tsai, M. C., S. Chakravarty, G. Zhu, J. Xu, K. Tanaka, C. Koch, J. Tufariello, J. Flynn, and J. Chan.** 2006. Characterization of the tuberculous granuloma in murine and human lungs: cellular composition and relative tissue oxygen tension. Cell Microbiol. **8:**218–232.
39. **Turner, O. C., R. J. Basaraba, A. A. Frank, and I. M. Orme.** 2003. Granuloma formation in mice and guinea pig models of experimental tuberculosis, p. 65–84. *In* D. L. Boros (ed.), Granulomatous infections and inflammation: cellular and molecular mechanisms. ASM Press, Washington, DC.
40. **Tyagi, S., E. Nuermberger, T. Yoshimatsu, K. Williams, I. Rosenthal, N. Lounis, W. Bishai, and J. Grosset.** 2005. Bactericidal activity of the nitroimidazopyran PA-824 in a murine model of tuberculosis. Antimicrob. Agents Chemother. **49:**2289–2293.
41. **Ulrichs, T., and S. H. Kaufmann.** 2006. New insights into the function of granulomas in human tuberculosis. J. Pathol. **208:**261–269.
42. **Ulrichs, T., M. Lefmann, M. Reich, L. Morawietz, A. Roth, V. Brinkmann, G. A. Kosmiadi, P. Seiler, P. Aichele, H. Hahn, V. Krenn, U. B. Gobel, and S. H. Kaufmann.** 2005. Modified immunohistological staining allows detection of Ziehl-Neelsen-negative *Mycobacterium tuberculosis* organisms and their precise localization in human tissue. J. Pathol. **205:**633–640.
43. **Wayne, L. G., and L. G. Hayes.** 1996. An in vitro model for sequential study of shiftdown of *Mycobacterium tuberculosis* through two stages of nonreplicating persistence. Infect. Immun. **64:**2062–2069.
44. **World Health Organization.** 2006. Report WHO/HTM/TB/2006.375. World Health Organization, Geneva, Switzerland.
45. **Yamazaki, Y., L. Danelishvili, M. Wu, E. Hidaka, T. Katsuyama, B. Stang, M. Petrofsky, R. Bildfell, and L. E. Bermudez.** 2006. The ability to form biofilm influences *Mycobacterium avium* invasion and translocation of bronchial epithelial cells. Cell Microbiol. **8:**806–814.
46. **Yamazaki, Y., L. Danelishvili, M. Wu, M. Macnab, and L. E. Bermudez.** 2006. *Mycobacterium avium* genes associated with the ability to form a biofilm. Appl. Environ. Microbiol. **72:**819–825.
47. **Zambrano, M. M., and R. Kolter.** 2005. Mycobacterial biofilms: a greasy way to hold it together. Cell **123:**762–764.